Progress In Electromagnetics Research Letters, Vol. 45, 89–98, 2014

Surface Plasmon Wave Manipulated by Quantum Coherence of Multilevel Quantum Dots

Jian Qi Shen [1, 2, *]

Abstract—An EIT (electromagnetically induced transparency)-based prism coupler is suggested for realizing tunable reflection spectrum via quantum coherence of phases in a multilevel system, where destructive and constructive quantum interference will occur among multilevel transition pathways that are driven by two external control fields. In this prism coupler, a semiconductor-quantum-dot (SQD) medium layer, which can exhibit EIT and relevant quantum coherent effects, bounds the prism base, and the two external control fields are used to manipulate the probe field and the excited surface plasmon wave (on the SQD layer surface). Then the surface plasmon wave modes, which are generated by the probe field incident into this multilevel SQD medium layer, can be coherently tunable through the switchable quantum interference (destructive and constructive quantum interference) among the energy levels in the SQD systems. Such switchable quantum interference can be realized if we tune the intensities (i.e., adjust a proper intensity ratio) of the two control fields that drive the SQD multilevel EIT system. New switchable photonic devices, which could find applications in photonic microcircuits as well as some areas in integrated optical circuits, could be designed based on this quantum-interference switchable surface plasmon resonance.

1. INTRODUCTION

Since surface plasmon excitation and SPR (surface plasmon resonance) polaritons can exhibit a strong interaction with nanoscopic objects, and would have many intriguing applications for designing new micro- and nano-scale photonic devices [1–3], recently the SPR optics have captured much interest in photonics, electronics and related technologies [4–9]. In the literature, an effect called ATR (attenuated total reflection), where surface plasmon resonance is involved, has been observed in Otto and Kretschmann's configurations (prism couplers) [10–12]. In such configurations, a sudden drawdown in the reflectance on the prism base is caused by the drastic coupling of incident waves into surface plasmon polariton modes in a thin metal layer, and hence the intensity of a p-polarized (TM) reflected wave exhibits a sharp dip when the angle of incidence at the prism base is larger than the total-reflection critical angle [13]. The ATR technique has been a powerful tool for determining metal characteristics (e.g., dielectric function and film thickness) [12–15], and the surface plasmon resonance (SPR) involved in has become a fundamental mechanism of many optical devices (e.g., optical sensors and modulators [16, 17]) and biomolecular sensors [18].

In order to offer working mechanisms for designing new photonic and quantum optical devices (e.g., logic and functional gates), phase coherence (quantum interference in multilevel transition pathways) can be one of the promising scenarios. For example, quantum-interference-based controllable SPR presented here would be particularly essential for the working principle of such photonic devices. We shall here suggest an experimentally feasible scheme, i.e., a prism coupling system (prism coupler) based

Received 11 December 2013, Accepted 14 March 2014, Scheduled 9 April 2014

* Corresponding author: Jian Qi Shen (jqshencn@gmail.com).

[1] Centre for Optical and Electromagnetic Research, State Key Laboratory of Modern Optical Instrumentations, East Building No. 5, Zijingang Campus, Zhejiang University, Hangzhou 310058, China. [2] Joint Research Centre of Photonics of the Royal Institute of Technology (Sweden) and Zhejiang University, Zijingang Campus, Zhejiang University, Hangzhou 310058, China.

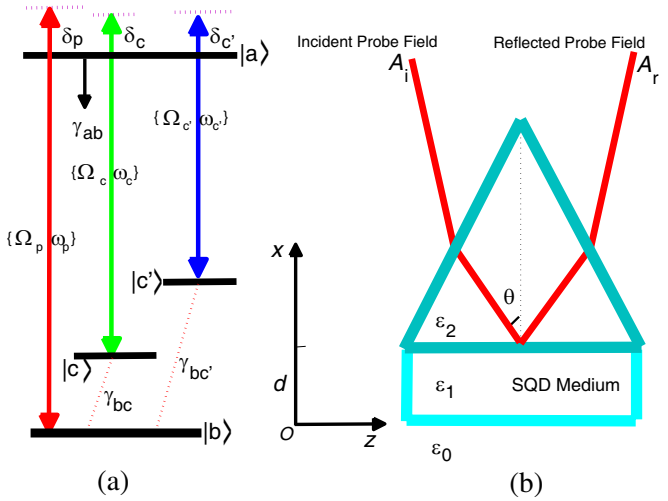

Figure 1. The schematic diagrams of (a) a four-level quantum coherent SQD system and (b) an EIT-prism coupler. The four-level quantum coherent system (an SQD multilevel system) is driven by two strong control fields and one weak probe field. The two control fields excite the $|c\rangle$-$|a\rangle$ and the $|c'\rangle$-$|a\rangle$ transitions, respectively. The probe wave that can excite the $|b\rangle$-$|a\rangle$ transition is incident and then reflected at the prism base, i.e., the interface (at $x = d$) between the prism dielectric and the thin EIT layer (SQD medium). The optical response of the $|b\rangle$-$|a\rangle$ transition can be coherently controlled by the destructive and constructive quantum interference between $|c\rangle$-$|a\rangle$ and $|c'\rangle$-$|a\rangle$ transitions.

on EIT (electromagnetically induced transparency) (see Fig. 1 for its schematic diagram) for achieving such an effect of quantum-interference-assisted surface plasmon excitation. In this EIT-prism coupler, an incident probe wave, which can be coupled into surface plasmon wave modes, will be dramatically influenced by the quantum interference between $|c\rangle$-$|a\rangle$ and $|c'\rangle$-$|a\rangle$ transitions driven by two control fields in a four-level EIT system (see Fig. 1(a)). Such a four-level EIT system can be found in a semiconductor-quantum-dot (SQD) system [19–21]. A quantum coherent medium layer, e.g., the four-level SQD medium layer, bounds the prism base (see Fig. 1(b)) in the present EIT-prism coupler for generating surface plasmon wave excitation. Then the surface plasmon wave will be excited underneath the quantum coherent SQD medium layer (at $x = 0$ plane).

In the sections that follow, we shall treat the optical behavior of the four-level semiconductor-quantum-dot medium and the electromagnetic eigenstates in the present EIT-prism coupler. The quantum-interference assisted tunable reflection spectrum will be given as an illustrative example for the application of the present EIT-prism coupler. The field distribution of optical excitation of surface plasmon wave, which can be controlled by the switchable quantum interference (SQD phase coherence) among the energy levels in the SQD system, will also be presented. We will conclude this work with some remarks on its potential applications in new photonic device design.

2. OPTICAL RESPONSE OF A FOUR-LEVEL SQD MEDIUM

Let us consider the optical response of the four-level SQD system required in our scenario of quantum-interference-based controllable SPR. The four-level SQD system $\{|a\rangle, |b\rangle, |c\rangle, |c'\rangle\}$ (see Fig. 1(a) for its energy level configuration) interacts with three laser beams, i.e., the two control fields and one probe field couple the level pairs $|c\rangle$-$|a\rangle$, $|c'\rangle$-$|a\rangle$ and $|b\rangle$-$|a\rangle$, respectively. Here, the three Rabi frequencies are expressed by $\Omega_c = \wp_{ac}E_c/\hbar$, $\Omega_{c'} = \wp_{ac'}E_{c'}/\hbar$, and $\Omega_p = \wp_{ab}E_p/\hbar$ with $\wp_{ac}$, $\wp_{ac'}$, and $\wp_{ab}$ the transition-induced electric dipole moments, and E_c, $E_{c'}$ and E_p the electric field envelopes (slowly varying amplitudes) of the strong control beams and the weak probe field, respectively. The three frequency detunings δ_c, $\delta_{c'}$ and δ_p are defined as follows: $\delta_c = \omega_c - \omega_{ac}$, $\delta_{c'} = \omega_{c'} - \omega_{ac'}$, and $\delta_p = \omega_p - \omega_{ab}$, where ω_{ac}, $\omega_{ac'}$ and ω_{ab} denote the energy-level transition frequencies, and ω_c, $\omega_{c'}$, ω_p represent the mode frequencies of the control and probe beams, respectively. The $|b\rangle$-$|a\rangle$ transition (driven by the

probe wave) can be controllably manipulated via the destructive and constructive quantum interference between $|c\rangle$-$|a\rangle$ and $|c'\rangle$-$|a\rangle$ transitions. If, for example, the destructive quantum interference between $|c\rangle$-$|a\rangle$ and $|c'\rangle$-$|a\rangle$ transitions occurs, the two levels $|c\rangle$ and $|c'\rangle$ seem to be *absent*, and then the four-level system $\{|a\rangle, |b\rangle, |c\rangle, |c'\rangle\}$ will be equivalent to a two-level one $\{|a\rangle, |b\rangle\}$.

We assume the Rabi frequency Ω_p of the probe field is sufficiently weak (i.e., it is small compared with the other parameters such as the spontaneous emission decay rate γ_{ab} and the control-field Rabi frequencies Ω_c, $\Omega_{c'}$), so that nearly all the SQDs remain in the ground state [22]. The electric polarizability of the SQD due to the probe transition $|b\rangle$-$|a\rangle$ is given by

$$\varrho = \frac{2\wp_{ba}\rho_{ab}}{\epsilon_0 E_p} = \frac{2|\wp_{ba}|^2\rho_{ab}}{\epsilon_0\hbar\Omega_p}. \tag{1}$$

By using the density matrix equation of the four-level system [23, 24], one can obtain the explicit expression for the microscopic electric polarizability of the SQD

$$\varrho = -\frac{|\wp_{ab}|^2}{\epsilon_0\hbar}\frac{(\delta_p - \delta_c + \mathrm{i}\gamma_{bc})(\delta_p - \delta_{c'} + \mathrm{i}\gamma_{bc'})}{\mathcal{D}} \tag{2}$$

with

$$\mathcal{D} = (\delta_p - \delta_c + \mathrm{i}\gamma_{bc})(\delta_p - \delta_{c'} + \mathrm{i}\gamma_{bc'})(\delta_p + \mathrm{i}\gamma_{ab}) - \frac{1}{4}\Omega_c^*\Omega_c(\delta_p - \delta_{c'} + \mathrm{i}\gamma_{bc'}) - \frac{1}{4}\Omega_{c'}^*\Omega_{c'}(\delta_p - \delta_c + \mathrm{i}\gamma_{bc}). \tag{3}$$

According to the Clausius-Mossotti relation that accounts for the contribution of all neighboring SQDs to the polarization of a given SQD system (local field correction), the relative electric permittivity of the SQD medium layer (i.e., the medium 1 in Fig. 1(b)) is given by $\varepsilon_1 = 1 + \frac{N\varrho}{1 - \frac{N\varrho}{3}}$ with N the concentration (total SQD number per unit volume) in the quantum coherent (EIT) medium. The typical parameters for the four-level SQD system are chosen as follows: the spontaneous emission decay rate $\gamma_{ab} = 1.0 \times 10^{10}\,\mathrm{s}^{-1}$ [19, 20], the collisional dephasing rates $\gamma_{bc} = \gamma_{ab}/50$, $\gamma_{bc'} = \gamma_{ab}/25$ [21], the electric dipole moment $\wp_{ab} = 6.3 \times 10^{-28}\,\mathrm{C}\cdot\mathrm{m}$ [19, 25], the Rabi frequency of one of the control field $\Omega_{c'} = 6.0\gamma_{ab}$ (the other Rabi frequency Ω_c will be tuned in order to realize *destructive* and *constructive* quantum interference), the detuning frequencies $\delta_{c'} = -0.4\gamma_{ab}$, $\delta_c = 1.2\gamma_{ab}$, and the SQD number density $N = 1.0 \times 10^{21}\,\mathrm{m}^{-3}$ [19, 26]. These parameters will be adopted throughout this work.

We shall point out that the electric permittivity ε_1 of the four-level quantum coherent SQD medium layer can have a negative real part (e.g., $\mathrm{Re}\varepsilon_1 = -7.5$, $\mathrm{Im}\varepsilon_1 = 2.2$) if the four-level system experiences destructive quantum interference between $|c\rangle$-$|a\rangle$ and $|c'\rangle$-$|a\rangle$ transitions when the Rabi frequency $\Omega_c = 5.0\gamma_{ab}$, and the electric permittivity ε_1 will have a small imaginary part (e.g., $\mathrm{Re}\varepsilon_1 = 1.5$, $\mathrm{Im}\varepsilon_1 = 0.02$) if the constructive quantum interference between $|c\rangle$-$|a\rangle$ and $|c'\rangle$-$|a\rangle$ transitions occurs when the Rabi frequency $\Omega_c = 18.0\gamma_{ab}$. This, therefore, means that under certain proper conditions (particularly in the case of destructive quantum interference), there will be surface plasmon wave excitations at the interface (at $x = 0$ plane) between the EIT layer and the bounding medium (located in the region of $x < 0$ shown in Fig. 1(b)). This will be demonstrated in more details in our numerical example.

3. AN EIT-PRISM COUPLER AND ITS REFLECTION SPECTRUM

Now we shall present the theoretical mechanism of the EIT-prism coupler, including the optical response of the tunable reflection spectrum and the field distribution (determined by the boundary conditions on the two sides of the SQD EIT layer) in the prism coupler. With the help of the Maxwell equations, the spatial distribution of the magnetic field in the prism system can be expressed as [12, 27]

$$H_y(x) = \begin{cases} A_i e^{\alpha_2(x-d)} + A_r e^{-\alpha_2(x-d)}, & x > d \\ A_1 e^{\alpha_1 x} + B_1 e^{-\alpha_1 x}, & 0 < x < d \\ A_0 e^{\alpha_0 x}, & x < 0 \end{cases} \tag{4}$$

where $\alpha_j = (\beta^2 - k_0^2\varepsilon_j^*)^{1/2}$ ($j = 0, 1, 2$ represents the bounding medium, the EIT medium and the prism dielectric, respectively) and the $\hat{z}$-direction phase constant $\beta = k_0\sqrt{\varepsilon_2^*}\sin\theta$ (the wave number in

vacuum is given by $k_0 = \omega/c$). Here, ε_j^* denotes the complex conjugate of ε_j because we will adopt the *convention of engineers* for the factor of phasor time dependence $e^{i\omega t}$ [28, 29] when we treat the field distribution in the prism coupler. By substituting Eq. (4) into the electromagnetic boundary conditions (i.e., the tangential components of the electric and magnetic fields are respectively continuous at the interfaces at $x = 0$ and $x = d$ in Fig. 1(a)), we can obtain the magnetic field amplitudes:

$$A_1 = \frac{1}{2}A_0\left(1 + \frac{\varepsilon_1^*\alpha_0}{\varepsilon_0^*\alpha_1}\right), \quad B_1 = \frac{1}{2}A_0\left(1 - \frac{\varepsilon_1^*\alpha_0}{\varepsilon_0^*\alpha_1}\right), \tag{5}$$

and

$$A_i = \frac{1}{2}\left[A_1 e^{\alpha_1 d}\left(1 + \frac{\varepsilon_2^*\alpha_1}{\varepsilon_1^*\alpha_2}\right) + B_1 e^{-\alpha_1 d}\left(1 - \frac{\varepsilon_2^*\alpha_1}{\varepsilon_1^*\alpha_2}\right)\right],$$

$$A_r = \frac{1}{2}\left[A_1 e^{\alpha_1 d}\left(1 - \frac{\varepsilon_2^*\alpha_1}{\varepsilon_1^*\alpha_2}\right) + B_1 e^{-\alpha_1 d}\left(1 + \frac{\varepsilon_2^*\alpha_1}{\varepsilon_1^*\alpha_2}\right)\right].$$

We will show how the quantum-interference switchable reflection spectrum can be coherently controlled by the two external control fields (these two control fields drive the $|c\rangle$-$|a\rangle$ and $|c'\rangle$-$|a\rangle$ transitions and hence the quantum interference between $|c\rangle$-$|a\rangle$ and $|c'\rangle$-$|a\rangle$ transition pathways can control the $|b\rangle$-$|a\rangle$ transition excited by the weak probe field). The reflectance of an electromagnetic wave (e.g., a weak TM probe wave) on the prism base is given by $R \equiv |A_r/A_i|^2$ with A_r and A_i the incident and reflected amplitudes, respectively. The wave vector of the incident probe field in the $\hat{z}$-direction (parallel to the prism-EIT interface) in this EIT-prism coupler can be equal to the wave vector of the surface plasmon wave if we tune the angle of incidence of the probe wave on the prism base at $x = d$ (i.e., the interface between the prism base and the thin SQD EIT medium layer). Such a surface plasmon wave mode can then be excited at the interface (at $x = 0$ underneath the SQD medium layer) if we choose a proper thickness d of the SQD medium layer. In other words, the EIT-prism system couples the incident probe wave into a surface plasmon wave mode. As a result, the reflectance at the prism base (the $x = d$ plane) decreases dramatically (e.g., the curve of the reflectance R at the incidence angle

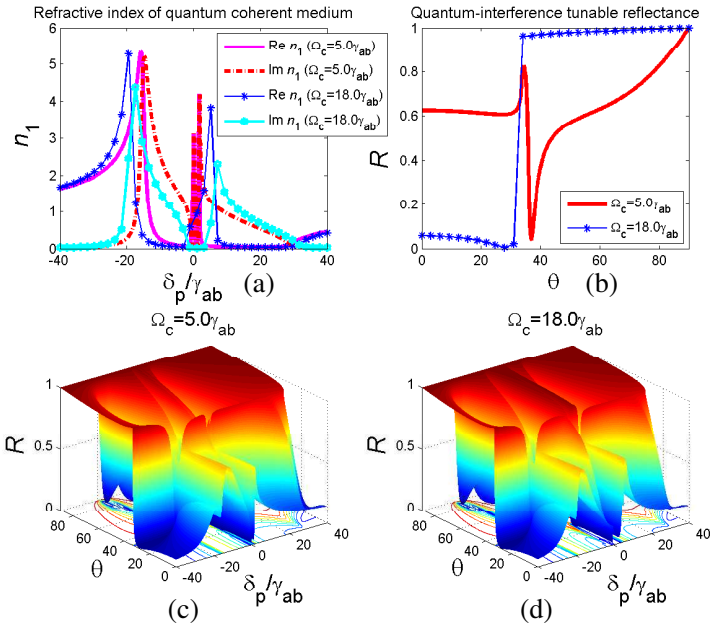

Figure 2. The dispersion characteristics of the refractive index of the four-level quantum coherent SQD medium and the quantum-interference switchable reflection spectrum of the EIT-prism coupler. In the curves of the reflectance R shown in (b), the probe frequency detuning is chosen as $\delta_p = 2.0\gamma_{ab}$.

$\theta \simeq 38^\circ$ when $\Omega_c = 5.0\gamma_{ab}$ in Fig. 2(b)). We choose the thickness of the SQD medium layer $d = 50\,\text{nm}$, the relative electric permittivity of the prism dielectric (i.e., medium 2 shown in Fig. 1(b)) $\varepsilon_2 = 3.24$, and the wavelength of the incident light in vacuum $\lambda = 632.8\,\text{nm}$ [14, 27]. In the region of $x < 0$ the dielectric (medium 0) is air (i.e., the relative permittivity $\varepsilon_0 = 1$). In what follows, we shall consider the dispersion characteristics and tunable behavior of the reflection spectrum of the prism coupler. Since the SQD-state phase interference is determined by the parameters: Ω_c (the strong control-field Rabi frequency) and δ_p (the weak probe frequency detuning), including the ratio $\Omega_c/\Omega_{c'}$, we shall consider the behavior of dependance of the reflection spectrum on these parameters.

The reflection spectrum depending upon the angle of incidence, θ, of the probe field on the prism base is presented in Figs. 2(b), (c), (d) and Fig. 3, where two representative cases, i.e., double-control *destructive* quantum interference (e.g., $\Omega_c = 5.0\gamma_{ab}$) and double-control *constructive* interference (e.g., $\Omega_c = 18.0\gamma_{ab}$), have been considered. In the case of double-control constructive interference (i.e., $\Omega_c = 18.0\gamma_{ab}$), the relative permittivity ε_1 of the SQD medium layer has a relatively small imaginary part (if δ_p is close to $\delta_{c'}$, then the imaginary part of the permittivity would be quite small because of the two-photon resonance and dark-state population trapping), and the reflectance R increases to 0.9 (close to that in total reflection) when the angle of incidence, θ, at the prism-EIT interface (at $x = d$) becomes large. For the case of destructive quantum interference (i.e., $\Omega_c = 18.0\gamma_{ab}$) between $|c\rangle$-$|a\rangle$ and $|c'\rangle$-$|a\rangle$ transitions, in which the permittivity ε_1 of the quantum coherent medium layer can exhibit some of the metal characteristics, e.g., ε_1 has a large negative real part and a relatively small imaginary part ($|\text{Re}\varepsilon_1| > \text{Im}\varepsilon_1$), the reflectance R is quite large (e.g., $R \simeq 0.6$) at small angle of incidence, and when $\theta > 30^\circ$, the reflectance R will increase quickly to 0.8, which is relevant to total reflection. Then when $\theta > 35^\circ$, R will, however, drops to a small value (almost zero). This is an effect of *attenuated total reflection*, since the surface plasmon resonance occurs at the lower interface (at $x = 0$) of the quantum coherent (EIT) medium layer, and the electromagnetic energy of the incident probe light has been coupled into this four-level SQD medium layer as a surface plasmon wave mode. In Fig. 3 the reflection spectrum in the narrow bands $[-20\gamma_{ab}, +20\gamma_{ab}]$ and $[-10\gamma_{ab}, +10\gamma_{ab}]$ of the probe frequency detuning δ_p is also presented in order to manifest more details of the dispersion characteristics of the reflection spectrum of this quantum-interference-assisted prism coupler.

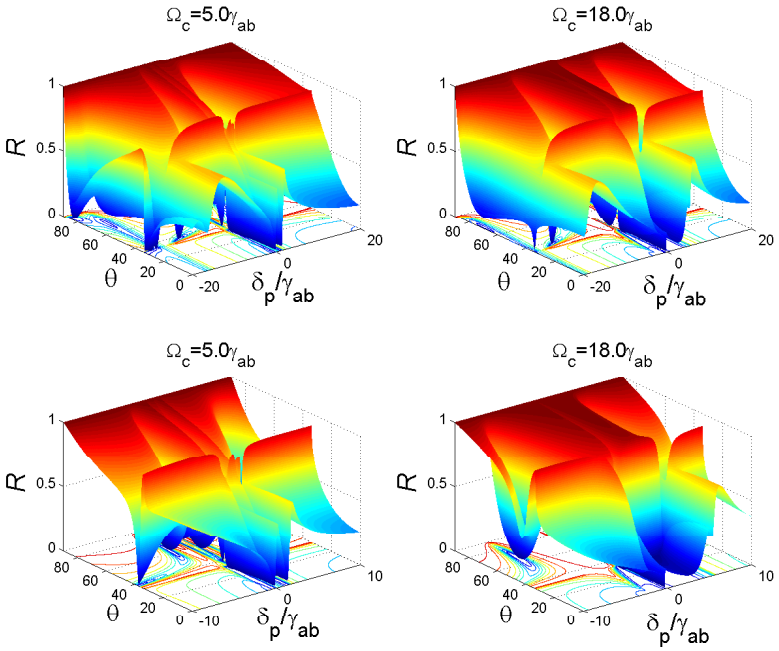

Figure 3. The dispersion characteristics of the quantum-interference switchable reflection spectrum of the EIT-prism coupler when the Rabi frequency $\Omega_c = 5.0\gamma_{ab}$ (destructive quantum interference) and $\Omega_c = 18.0\gamma_{ab}$ (constructive quantum interference).

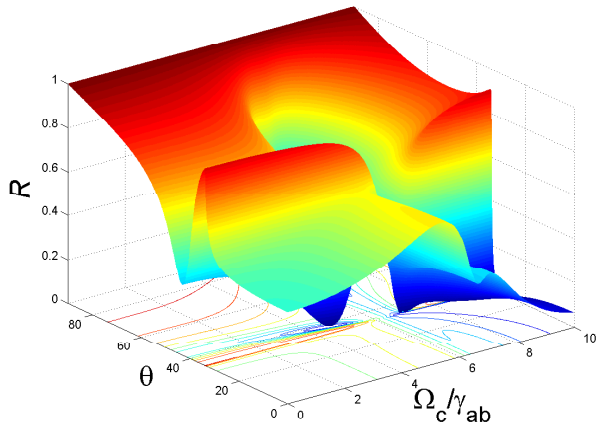

Figure 4. The tunable reflection spectrum when the control-field Rabi frequency Ω_c changes. The frequency detuning of the incident probe field is $\delta_p = 2.0\gamma_{ab}$. The reflectance R decreases to zero at some positions, e.g., $\Omega_c = 5.0\gamma_{ab}$ and $\theta = 37°$, which will be considered in more details.

The tunable reflection spectrum depending upon the control-field Rabi frequency Ω_c is presented in Fig. 4. Since the EIT system experiences constructive quantum interference between $|c\rangle$-$|a\rangle$ and $|c'\rangle$-$|a\rangle$ transitions (driven by the two control fields) when Ω_c is in the range $[6.0\gamma_{ab}, 10.0\gamma_{ab}]$, the four-level SQD medium has a small imaginary part in the permittivity ε_1. Therefore, the reflectance R is small at $\theta = 0°$ because the incident light is highly transmitted into the EIT medium layer. But when $\Omega_c < 6.0\gamma_{ab}$, the destructive quantum interference between $|c\rangle$-$|a\rangle$ and $|c'\rangle$-$|a\rangle$ transitions would take place. Then it seems that both the two levels $|c\rangle$, $|c'\rangle$ and the two control fields Ω_c, $\Omega_{c'}$ were absent. In this case, the SQD medium permittivity has a large imaginary part, and the incident light is highly reflected on the interface (prism base) at small angles of incidence (this is similar to the case of incidence on a metal surface). In all these ranges of Ω_c, the reflectance R is always increasing when θ becomes large. But there are some ranges of the incidence angle θ for R to become small (or almost zero) due to surface plasmon resonance that couples the incident light into the thin layer of the four-level SQD medium. In other words, when $\theta > 30°$, the total reflection should have already taken place, but now instead, it has actually been replaced by the effect of *attenuated total reflection* (i.e., the reflectance drops to zero) due to the surface plasmon wave excitation (at $x = 0$ plane). Such a process of surface wave excitation is coherently induced by the quantum interference in the four-level SQD system.

4. OPTICAL EXCITATION OF SURFACE PLASMON WAVE MODES IN THE PRISM COUPLER

In the preceding section, we have considered the tunable reflection spectrum, where the reflectance R decreases to zero when the surface plasmon wave is excited. Now we shall treat the issue of optical excitation of surface plasmon wave modes in the prism coupler. The field distribution at the interface between a medium and the quantum coherent SQD layer is shown in Fig. 5 (the incidence angle of the probe field on the prism base is $\theta = 38°$) and in Fig. 6 (the incidence angle $\theta = 37°$). Here, the Rabi frequency of the control field driving the $|c\rangle$-$|a\rangle$ transition is $\Omega_c = 5.0\gamma_{ab}$ (i.e., corresponding to the destructive quantum interference). The relative permittivity of the quantum coherent SQD medium layer (corresponding to the case of $\Omega_c = 5.0\gamma_{ab}$) is $\varepsilon_1 = -7.5 + 2.2\mathrm{i}$. It should be pointed out that there is no surface plasmon wave excited at the interface of $x = 0$ when the incidence angle θ is 38° (see in Fig. 5, where the field amplitude at the interface of $x = 0$ is almost equal to the incident amplitude of the probe field). But when the angle of incidence of the probe field on the prism base is $\theta = 37°$, the surface plasmon wave will be excited by the incident probe field. It can be seen from Fig. 6 that the field amplitude at the interface of $x = 0$ is larger than the incident amplitude of the probe field (the fact that *the amplitude excited at the interface is larger than that of the illuminating light* can be considered a visual criterion of surface plasmon wave excitation). Then the electromagnetic

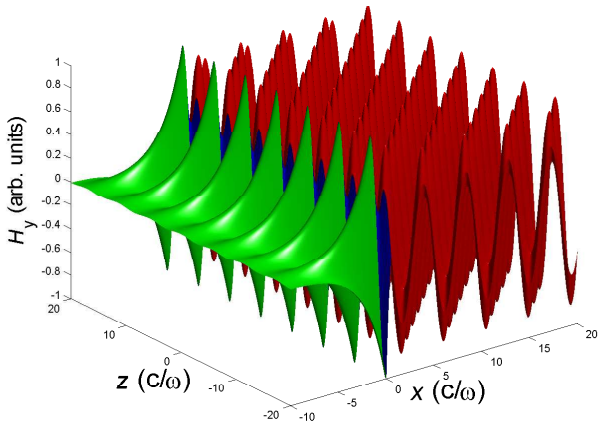

Figure 5. The electromagnetic eigen mode of surface wave propagates in the $\hat{z}$-direction parallel to the interface between the SQD medium layer ($x = [0, 50]$ nm) and the air medium ($x < 0$), and decays evanescently in the $\hat{x}$-direction perpendicular to the interface. The incidence angle $\theta = 38^{\circ}$.

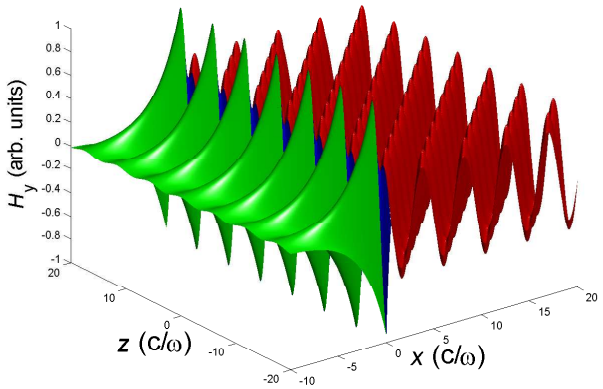

Figure 6. Optical excitation of a surface plasmon wave mode in the prism coupler when the incidence angle $\theta = 37^{\circ}$. The electromagnetic eigen mode of surface wave propagates in the $\hat{z}$-direction parallel to the interface between the SQD medium layer ($x = [0, 50]$ nm) and the air medium ($x < 0$), and decays evanescently in the $\hat{x}$-direction perpendicular to the interface.

excitation (a surface eigen mode of the Maxwell equations) propagates in the $\hat{z}$-direction parallel to the layer interface of the quantum coherent SQD medium, and decays evanescently in the perpendicular direction to the interface. It can be found that the attenuation length in the $\hat{x}$-direction in air (in the half space $x < 0$) is less than $5c/\omega \simeq \lambda$ (subwavelength strong confinement). Since the optical behavior of the quantum coherent medium depends upon the applied external control fields, we have so far shown that the attenuation length of the surface wave modes due to strong localization can be controllably manipulated by SQD phase coherence (destructive and constructive quantum interference among multilevel transition pathways driven by external control fields).

5. DISCUSSIONS

We shall discuss the topics concerning the effects of inhomogeneous broadenings on quantum dots, and suggest how to reduce the impact, and then present a brief prescription to treat the effects due to homogeneous and inhomogeneous broadenings:

The homogeneous and inhomogeneous broadening effects on quantum dots have been considered by many authors [30–34]. When the self-assembled quantum dots are formed, it will exhibit inhomogeneous

broadening because of nonuniformity of size (size fluctuations) [32], strain distribution, and material composition of quantum dots [30], and hence the signal and pump beams experience different detunings at different quantum dots (i.e., each frequency detuning depends on the individual quantum dot size) [25, 32]. Though each quantum dot can exhibit quantum coherence, the total contribution of all the quantum dots in one wavelength to quantum coherence will be cancelled. In the references, some routes have been suggested in order to reduce the impact of inhomogeneous broadening on quantum dots, e.g., resonant microcavity scenario [25] and multicolour pumping scheme [31]. Some authors suggested a simple scheme, i.e., if the coupling power density is large enough for Rabi splitting to overcome the inhomogeneous broadening width, the detrimental effect of inhomogeneous broadening would be suppressed [32].

If we do not adopt these routes for reducing the quantum dot size effects, the influence can also be analyzed by using some methods, e.g., *spatially resolved model* that can incorporate homogeneous and inhomogeneous broadenings for quantum dots [33]. In this model, different quantum dot sizes yield their own confined energies that can be calculated by solving the Schrodinger equation. A separate rate equation is assigned to each energy level as well as to each carrier type [33]. Here, the size distribution must be quantized into subgroups. Such size distribution subgroups can be determined in accordance with the energetic spacing between each group and its neighboring groups, where the homogeneously broadened line is also taken into account [33].

We shall close this section by illustrating the following performances of the EIT-based prism coupler for experimental verification:

i) *The quantum-interference switchable reflection spectrum.* The tunable reflection spectrum (depending upon the incidence angle θ) can be controllable manipulated by the quantum interference between $|c\rangle$-$|a\rangle$ and $|c'\rangle$-$|a\rangle$ transitions driven by the two control fields. The reflectance of the prism base is determined by the intensity ratio of the two control fields.

ii) *Surface plasmon wave excitation.* When the four-level SQD system experiences destructive quantum interference between $|c\rangle$-$|a\rangle$ and $|c'\rangle$-$|a\rangle$ transitions and the incident probe light illuminates the prism base at a proper incidence angle, the surface plasmon wave will be drastically excited in the thin SQD layer (enhancement of light-atom interaction).

iii) *Extremely dispersion-sensitive optical response of both tunable reflection spectrum and surface plasmon wave excitation.* The dispersion (close to the resonance frequency) in the permittivity of the multilevel medium is strong, e.g., 10^5 times that in a metal. Such a dispersion-ultrasensitive behavior of multilevel medium is also the physical origin of slow light [25]. It can open opportunities for designing new optical and photonic devices that are sensitive to external fields.

6. CONCLUDING REMARKS

The EIT-based surface plasmon resonance presented here has three attractive characteristics: i) the switchable quantum interference is exhibited by surface plasmon wave excitation, ii) the surface plasmon resonance is quantum-coherently manipulated by external control fields, iii) the surface plasmon wave is quite sensitive to dispersion of the quantum coherent medium. Since the optical response of a four-level SQD system can be controllably manipulated via tunable quantum interference between level transitions driven by two control fields, the double-control quantum interference can lead to various nontrivial interference-switchable optical behavior. By taking full advantage of such a multilevel SQD optical response, the quantum-interference switchable effect of *attenuated total reflection* accompanied by surface plasmon resonance can be utilized to design some new photonic logic and functional gates (e.g., the two applied control fields act as input signals in these gate devices) as well as sensitively switchable devices, which could find new applications in all-optical technique, photonic microcircuits (and integrated optical circuits).

ACKNOWLEDGMENT

This work is supported in part by the National Natural Science Foundation of China under Grants Nos. 11174250, 91233119, 60990320, and the Program of Zhejiang Leading Team of Science and Technology Innovation.

REFERENCES

1. Barnes, W. L., A. Dereux, and T. W. Ebbesen, "Surface plasmon subwavelength optics," *Nature*, Vol. 424, 824–830, 2003.
2. Ozbay, E., "Plasmonics: Merging photonics and electronics at nanoscale dimensions," *Science*, Vol. 311, 189–193, 2006.
3. Yoon, J., S. H. Song, and J.-H. Kim, "Extraction efficiency of highly confined surface plasmon-polaritons to far-field radiation: An upper limit," *Opt. Express*, Vol. 16, 1269–1279, 2008.
4. Shin, H. and S. Fan, "All-angle negative refraction for surface plasmon waves using a metal-dielectric-metal structure," *Phys. Rev. Lett.*, Vol. 96, 073907, 2006.
5. Kim, H., J. Park, and B. Lee, "Tunable directional beaming from subwavelength metal slits with metal-dielectric composite surface gratings," *Opt. Lett.*, Vol. 34, 2569–2571, 2009.
6. Mueckstein, R. and O. Mitrofanov, "Imaging of terahertz surface plasmon waves excited on a gold surface by a focused beam," *Opt. Express*, Vol. 19, 3212–3217, 2011.
7. Zhang, J., S. Xiao, M. Wubs, and N. A. Mortensen, "Surface plasmon wave adapter designed with transformation optics," *ACS Nano.*, Vol. 5, 4359–4364, 2011.
8. Zhong, R.-B., W. -H. Liu, J. Zhou, and S.-G. Liu, "Surface plasmon wave propagation along single metal wire," *Chin. Phys. B*, Vol. 21, 117303, 2012.
9. Norrman, A., T. Setälä, and A. T. Friberg, "Exact surface-plasmon polariton solutions at a lossy interface," *Opt. Lett.*, Vol. 38, 1119–1121, 2013.
10. Otto, A., "Excitation of non-radiative surface plasma waves in silver by the method of frustrated total reflection," *Z. Phys.*, Vol. 216, 398–410, 1968.
11. Kretschmann, E., "The determination of the optical constants of metals by excitation of surface plasmons," *Z. Phys.*, Vol. 241, 313–324, 1971.
12. Ding, Y., Z. Q. Cao, and Q. S. Shen, "Improved SPR technique for determination of the thickness and optical constants of thin metal films," *Opt. Quantum Electron.*, Vol. 35, 1091–1097, 2003.
13. Ishimaru, A., S. Jaruwatanadilok, and Y. Kuga, "Generalized surface plasmon resonance sensors using metamaterials and negative index materials," *Progress In Electromagnetics Research*, Vol. 51, 139–152, 2005.
14. Weber, W. H. and S. L. McCarthy, "Surface-plasmon resonance as a sensitive optical probe of metal-film properties," *Phys. Rev. B*, Vol. 12, 5643–5650, 1975.
15. Regalado, L. E., R. Machorro, and J. M. Siqueiros, "Attenuated-total-reflection technique for the determination of optical constants," *Appl. Opt.*, Vol. 30, 3176–3180, 1991.
16. Homola, J., S. S. Yee, and G. Gauglitz, "Surface plasmon resonance sensors: Review," *Sens. Actuators B*, Vol. 54, 3–15, 1999.
17. Jiang, Y., Z. Cao, G. Chen, X. Dou, and Y. Chen, "Low voltage electro-optic polymer light modulator using attenuated total internal reflection," *Opt. Laser Technol.*, Vol. 33, 417–420, 2001.
18. Schuck, P., "Use of surface plasmon resonance to probe the equilibrium and dynamic aspects of interactions between biological macromolecules," *Annu. Rev. Biophys. Biomol. Struct.*, Vol. 26, 541–566, 1997.
19. Jänes, P., J. Tidström, and L. Thylén, "Limits on optical pulse compression and delay bandwidth product in electromagnetically induced transparency media," *J. Lightwave Tech.*, Vol. 23, 3893–3899, 2005.
20. Mathew R., C. E. Pryor, M. E. Flatté, and K. C. Hall, "Optimal quantum control for conditional rotation of exciton qubits in semiconductor quantum dots," *Phys. Rev. B*, Vol. 84, 205322, 2011.
21. Arve, P., P. Jänes, and L. Thylén, "Propagation of two-dimensional pulses in electromagnetically induced transparency media," *Phys. Rev. A*, Vol. 69, 063809, 2004.
22. Scully, M. O. and M. S. Zubairy, *Quantum Optics*, Chap. 7, Cambridge University Press, Cambridge, England, 1997.
23. Paspalakis, E. and P. L. Knight, "Electromagnetically induced transparency and controlled group velocity in a multilevel system," *Phys. Rev. A*, Vol. 66, 015802, 2002.

24. Shen, J. Q. and P. Zhang, "Double-control quantum interferences in a four-level atomic system," *Opt. Express*, Vol. 15, 6484–6493, 2007.
25. Kim, J., S. L. Chuang, P. C. Ku, and C. J. Chang-Hasnain, "Slow light using semiconductor quantum dots," *J. Phys.: Condens. Matter*, Vol. 16, S3727–S3735, 2004.
26. Nielsen, P. K., H. Thyrrestrup, and B. Tromborg, "Numerical investigation of electromagnetically induced transparency in a quantum dot structure," *Opt. Express*, Vol. 15, 6396–6408, 2007.
27. Cao, Z. Q., *Optics of Guided Waves*, Chap. 9, Science Press of China, Beijing, 2007.
28. Yeh, P., *Optical Waves in Layered Media*, Chaps. 4–6, 83–143, John Wiley & Sons, Inc., New Jersey, USA, 2005.
29. Caloz, C. and T. Itoh, *Electromagnetic Metamaterials: Transmission Line Theory and Microwave Applications*, Chap. 2, John Wiley & Sons, Inc., New Jersey, USA, 2006.
30. Fu, Y., F. Ferdos, M. Sadeghi, S. M. Wang, and A. Larsson, "Photoluminescence of an assembly of size-distributed self-assembled InAs quantum dots," *J. Appl. Phys.*, Vol. 92, 3089–3092, 2002.
31. Chang-Hasnain, C. J., P. C. Ku, J. Kim, and S. L. Chuang, "Variable optical buffer using slow light in semiconductor nanostructures," *Proc. IEEE*, Vol. 9, 1884–1897, 2003.
32. Lunnemanna, P. and J. Mørk, "Reducing the impact of inhomogeneous broadening on quantum dot based electromagnetically induced transparency," *Appl. Phys. Lett.*, Vol. 94, 071108, 2009.
33. Gready, D. and G. Eisenstein, "Effects of homogeneous and inhomogeneous broadening on the dynamics of tunneling injection quantum dot lasers," *IEEE J. Quantum Electron.*, Vol. 47, 944–949, 2011.
34. Taleb, H. and K. Abedi, "Homogeneous and inhomogeneous broadening effects on static and dynamic responses of quantum-dot semiconductor optical amplifiers," *Front. Optoelectron.*, Vol. 5, 445–456, 2012.